HHS Public Access

Author manuscript

Oncogene. Author manuscript; available in PMC 2019 April 10.

Published in final edited form as:

Oncogene. 2019 February ; 38(9): 1576–1584. doi:10.1038/s41388-018-0523-6.

Leukemia Inhibitory Factor Functions in Parallel with Interleukin-6 to Promote Ovarian Cancer Growth

Karen McLean[1,*], **Lijun Tan**[1], **Danielle E. Bolland**[1], **Lan G. Coffman**[4], **Luke F. Peterson**[2], **Moshe Talpaz**[2], **Nouri Neamati**[3], and **Ronald J. Buckanovich**[4]

[1]Division of Gynecologic Oncology, Department of Obstetrics and Gynecology, University of Michigan Medical Center, Ann Arbor, MI

[2]Division of Hematology Oncology, Department of Internal Medicine, University of Michigan Medical Center, Ann Arbor, MI

[3]Department of Medicinal Chemistry, College of Pharmacy North Campus Research Complex, Ann Arbor, MI

[4]Magee-Womens Research Institute University of Pittsburgh School of Medicine, Pittsburg, PA

Abstract

Ovarian carcinoma-associated mesenchymal stem cells (CA-MSC) produce not only high levels of IL6 but also the related cytokine leukemia inhibitory factor (LIF). Interleukin 6 (IL6) mediated activation of STAT3 is implicated as a critical therapeutic target for cancer therapy. Less is known about the role of LIF, which can similarly activate STAT3, in ovarian cancer. We therefore sought to evaluate the tumorigenic effects of CA-MSC paracrine LIF signaling and the redundancy of IL6 and LIF in activating ovarian cancer STAT3 mediated cancer growth. As expected, we found that both IL6 and LIF induce STAT3 phosphorylation in tumor cells. In addition, both IL6 and LIF increased the percentage of ALDH+ ovarian cancer stem-like cells (CSC). Supporting redundancy of function by the two cytokines, CA-MSC induced STAT3 phosphorylation and increased cancer cell 'stemness'. This effect was not inhibited by LIF or IL6 blocking antibodies alone, but was prevented by dual IL6/LIF blockade or JAK2 inhibition. Similarly, small hairpin RNA (shRNA)-mediated reduction of IL6 or LIF in CA-MSC partially decreased but could not completely abrogate the ability of CA-MSC to induce STAT3 phosphorylation and stemness. Importantly, the in vivo pro-tumorigenic effect of CA-MSC is abrogated by dual blockade with the JAK2 inhibitor ruxolitinib to a much greater extent than treatment with anti-IL6 or anti-LIF antibody alone. Ruxolitinib treatment also improves survival in the immunocompetent ovarian cancer mouse model system with ID8 tumor cells plus MSC. Ruxolitinib-treated tumors in both the immunocompromised and immunocompetent animal models demonstrate decreased phospho-STAT3, indicating on-target activity. In conclusion, CA-MSC activate ovarian cancer cell STAT3 signaling via IL6 and LIF and increase tumorigenesis cancer stemness. This functional redundancy

[*]**Corresponding Author** Karen McLean, MD, PhD, University of Michigan, 1500 E. Medical Center Drive, Ann Arbor, MI 48109-5276, 734.615.3773 (phone) 734.764.7261 (fax), arenmcl@umich.edu.

Conflict of Interest: The authors have no conflicts of interest to disclose.

suggests that therapeutic targeting of a single cytokine may be less effective than strategies such as dual inhibitor therapy or targeting shared downstream factors of the JAK/STAT pathway.

Keywords

mesenchymal stem cells; ovarian cancer; leukemia inhibitory factor (LIF); interleukin-6 (IL6); STAT3; JAK2 inhibition; ID8

Introduction

Ovarian cancer is a disease plagued by recurrence and the development of chemoresistance. Despite significant efforts to improve patient outcomes, five-year survival for women with ovarian cancer remains approximately 50% [1]. New treatment strategies that reduce recurrence are essential. Increasing data indicate that the tumor microenvironment in ovarian cancer promotes tumor progression and resistance to therapy [18]. Mesenchymal stem cells (MSC) are multipotent cells in the tumor microenvironment with the capacity to differentiate into several microenvironment cell types including fibroblasts, myofibroblasts and adipocytes. These differentiated stromal cell types can promote tumor growth [12, 19]. Additionally, carcinoma associated fibroblasts have been shown to mediate ovarian cancer platinum resistance [26]. Thus, inhibiting microenvironment signaling is a potential new therapeutic approach for ovarian cancers and we are now challenged with identifying the ideal therapeutic targets for tumor microenvironment-directed treatments.

Our group has previously isolated and characterized carcinoma-associated mesenchymal stem cells (CA-MSC) from primary tumors of ovarian cancer patients [17]. These CA-MSC are multipotent cells that promote ovarian cancer tumor growth and chemotherapy resistance, and this effect is greater with CA-MSC than non-cancer adipose-derived MSC [5, 17]. We have therefore been working to define the mechanisms by which CA-MSC exert this pro-tumorigenic effect. We previously determined that increased bone morphogenic protein (BMP) signaling by CA-MSC is one such mechanism [17]. However, blockade of this pathway with the BMP inhibitor Noggin failed to completely abrogate the protumorigenic effects of CA-MSC, supporting the existence of additional critical signaling pathways. mRNA expression analysis demonstrated that both interleukin-6 (IL6) and the related cytokine leukemia inhibitory factor (LIF) are upregulated in CA-MSC compared to control MSC [17]. IL6 and LIF are secreted cytokines that bind to a transmembrane receptor that heterodimerizes with a shared receptor, GP130, on epithelial cells. This binding results in Janus kinase (JAK) activation and subsequent activating phosphorylation of signal transduces and activator of transcription 3 (STAT3). Within the epithelial cells STAT3 activation promotes cell survival and proliferation as well as cell migration [29]. Numerous studies suggest IL6-mediated STAT3 activation plays a critical role in tumor biology for ovarian and other solid cancers [29]. Increased serum IL6 levels are correlated with a poorer outcome in multiple cancer types including ovarian cancer [24]. Elevated IL6 levels in the ascites of ovarian cancer patients similarly predicts poor prognosis [16].

While the role of IL6 in carcinogenesis has been intensely studied, the role of LIF in solid cancer tumorigenesis is less well characterized. However, a critical role for LIF activated

STAT3 signaling has been proposed in glioblastoma, pancreatic and nasopharyngeal cancers [6, 13, 21]. Increased LIF expression has been shown to be correlated with advanced clinical stage and higher grade in both serous and mucinous ovarian cancers [28].

Due to the important role of JAK/STAT signaling in tumorigenesis, investigators have assessed the impact of blocking this pathway on ovarian cancer cell growth properties in vitro and in vivo. The JAK2 inhibitor AG490 has been shown suppress growth and induce apoptosis in ovarian cancer cells, as well as enhancing cisplatin mediated cell death [4]. The JAK2 inhibitor AZD1480 also leads to decreased ovarian cancer xenograft tumor growth and metastasis in mice [11]. Interestingly, in this animal model, fewer suppressor T cells were found in the tumor microenvironment of animals treated with the JAK2 inhibitor. We found the JAK2 inhibitor TG101209 reduced metastasis in a murine model of endometrioid ovarian cancer [3, 20]. Similarly, the STAT3 inhibitor HO-3867 has been shown to block ascites-mediated activation of STAT3 in ovarian cancer cells to inhibit cancer cell invasion and metastasis in both ex vivo cultures and an orthotopic mouse model [23].

Despite these encouraging studies on JAK/STAT pathway inhibition of epithelial ovarian cancer tumor cells, current efforts have largely failed to address the impact of the tumor microenvironment and particularly stromal cells on pathway activation. Murine IL6 does not activate the human IL6 receptor [25], thus murine xenograft models utilizing only human epithelial tumor cells do not assess the impact of the tumor microenvironment. Thus model systems that include both human tumor cells and human microenvironment cells are necessary. In addition to our work on CA-MSC, other studies support a role for tumor microenvironment signaling influencing cancer cell biology. Adipose stromal cells, which can be derived from CA-MSC, have been reported to enhance ovarian cancer cell migration through the IL6/JAK/STAT3 pathway [14]. IL6 secreted by CA-MSC has been shown to increase CSC and xenograft growth of the SKOV3 cell line [9].

We hypothesized that IL6 and LIF secreted in tumor microenvironment function in concert to activate ovarian cancer cell JAK-STAT signaling. Herein we present data demonstrating both IL6 and LIF are produced by CA-MSC, induce tumor cell JAK-STAT signaling, increase the percentage of cancer stemlike cells (CSC) in the epithelial cancer cell population, and promote tumor cell growth both in vitro and in vivo in xenograft models. As such, therapeutic blockade of common signaling cascade molecules is superior to individually blocking IL6 or LIF on decreasing the pro-tumorigenic effects of CA-MSC. These finding have significant implications for clinical trial design in the treatment of ovarian cancer.

Results and Discussion

Cancer-Associated MSC secrete IL6 and LIF to Induce Tumor Cell STAT3 Phosphorylation

We previously performed messenger RNA profiling comparing CA-MSC to non-cancer control MSC, using a human MSC PCR array [17]. Numerous factors known to activate the JAK-STAT pathway including IL-6 and LIF were noted to be upregulated in CA–MSC [17]. We therefore performed qRT-PCR to quantify the mRNA expression of IL-6 and LIF in CA-MSC and healthy donor adipose-derived control MSC. Compared to normal adipose-derived

MSC, CA-MSC demonstrated increased expression of both IL6 and LIF (Fig. 1A, 1B). Interestingly expression of these two cytokines was heterogeneous amongst samples. For example, CA-MSC derived from patient 200 demonstrated very high expression of IL-6 and modest expression of LIF, whereas CA-MSC derived from patients 122 and 134 demonstrated high expression of LIF and modest expression of IL-6 (Fig. 1A, B).

Given the expression of IL6 and LIF by CA-MSC, we evaluated the ability of CA-MSC conditioned media to induce STAT3 phosphorylation in the SKOV3 and OVCAR3 epithelial ovarian cancer cell lines. Although using SKOV3 cells as a model for high grade serous ovarian cancer is controversial [10], these cell lines were chosen as they have a low level of basal STAT3 phosphorylation and have been extensively studied in the ovarian cancer literature [10]. Treatment of ovarian cancer cells with CA-MSC conditioned media resulted in an increase in STAT3 phosphorylation (Fig. 2A, 2D). Treatment with either IL6 or LIF blocking antibodies reduced STAT3 phosphorylation in ovarian cancer cells exposed to CA-MSC conditioned media, suggesting both IL6 and LIF contribute to STAT3 phosphorylation (Fig. 2A). Furthermore, dual IL6 and LIF blockade resulted in near complete elimination of STAT3 phosphorylation (Fig 2A). Together these data suggest that IL6 and LIF may function in a parallel manner to activate STAT3 signaling.

We next sought to assess the effect of inhibiting downstream common signaling cascade proteins JAK2 or STAT3 on the ability of CA–MSC conditioned media to induce phosphorylation of STAT3. Multiple inhibitors were initially investigated, including the STAT3 inhibitor Stattic and the JAK2 inhibitors TG101209 and ruxolitinib [30]. The JAK2 inhibitor TG101209 demonstrated near complete blockade of IL6 and LIF mediated induction of phosphorylation of STAT3 in contrast to limited efficacy of the STAT3 inhibitor Stattic (Fig. 2B). The JAK2 inhibitor ruxolitinib resulted in complete inhibition of STAT3 phosphorylation in multiple cell lines including SKOV3 and OVCAR3 (Fig. 2C, 2D). Similar to dual antibody blockade, ruxolitinib was shown to block CA-MSC conditioned media mediated phosphorylation of STAT3 in ovarian cancer cell lines (Fig. 2D).

IL6 and LIF from Cancer-Associated MSC Increase Cancer Stem-Like Cells

We previously demonstrated that CA-MSC increase the percentage of $ALDH^+$ ovarian cancer stem-like cells (CSC) [17]. IL6 can increase the CSC population in breast cancer [15]. We therefore tested the impact of IL6 and LIF on CSC population in ovarian cancer cell lines using both sphere assays and flow cytometric quantification of $ALDH^+$ ovarian cancer cells. We first performed tumor sphere assays. Both IL6 and LIF treatment increase the number of ovarian tumor spheres formed (Fig. 3A). Supporting redundancy of the two cytokines, LIF promoted tumor sphere growth in the presence of IL-6 blockade, and IL6 promoted tumor sphere growth in the presence of LIF blockade (Fig. 3A). Furthermore, the treatment with both recombinant cytokines and blockade of only one cytokine still resulted in a statistically significant induction of spheres as compared to the basal level, highlighting the critical role of both cytokines in increasing CSC. Dual blockade of IL6 and LIF with either blocking antibodies or inhibition of the shared cytokine receptor GP130 with SC144 [27] suppressed tumor sphere formation (Fig. 3A and 3B). These studies were then extended to primary tumor cells, with the finding that recombinant IL6 and LIF increase sphere formation by

tumor cells derived from patient ascites, and this effect is blocked by the addition of ruxolitinib (Fig. 3C). We then confirmed our results by measuring the percentage of $ALDH^+$ cells following cytokine treatment and blockade. We found that both IL6 and LIF induce an increase in the percentage of $ALDH^+$ CSC as quantified by flow cytometry in SKOV3 and OVCAR3 cell lines (Fig. 3D and data not shown). Ruxolitinib successfully blocked IL6 and LIF induction of $ALDH^+$ CSC (Fig. 3D).

To further characterize the role of CA-MSC secreted IL6 and LIF on both the induction of STAT3 phosphorylation and increase in tumor CSC, knockdown experiments were also performed. Small hairpin RNA (shRNA) methodology was utilized to decrease IL6 and LIF levels in CA-MSC. The ability of the shRNA constructs to decrease CA-MSC IL6 and LIF levels was verified by immunoblotting (Fig. 3E). SKOV3 ovarian cancer cells were then treated with conditioned media from shRNA control or shRNA knockdown CA-MSC. We found that shRNA-mediated knockdown of IL6 or LIF in the CA-MSC lessened the ability of CA-MSC conditioned media to induce STAT3 phosphorylation (Fig. 3F) and decreased CAMSC mediated induction of CSC as quantified by the percentage of $ALDH^+$ cells (Fig. 3G).

IL6/LIF blockade inhibits the Protumorigenic Effects of CA-MSC in vivo

We previously demonstrated CA-MSC significantly promote tumor growth in vivo [17]. We next sought to determine in vivo the relative effects of individual cytokine blockade with antibody therapy compared to dual blockade with the JAK2 inhibitor ruxolitinib. Ruxolitinib was selected for in vivo study given that Federal Drug Administration approval has already been achieved in hematologic diseases. Tumor xenografts were generated using OVCAR3 epithelial ovarian cancer cells and CA-MSC to provide a human ovarian cancer stromal microenvironment [5]. Treatment with anti-IL6 antibody tocluzimab or anti-LIF antibody resulted in a statistically significant decrease in tumor growth as compared to untreated controls (Fig. 4A). Ruxolitinib therapy decreased tumor growth to a greater extent than either individual antibody therapy and significantly decreased final tumor mass (Fig. 4A, 4B).

To confirm on target activity of the drugs, phosphorylated STAT3 levels in the tumors were assessed by immunoblotting. Ruxolitinib therapy resulted an approximately 70 percent decrease in phospho-STAT3 levels in comparison to untreated control tumors, while anti-IL6 or anti-LIF therapy alone had no significant impact on phospho-STAT3 levels (Fig. 4C). Finally, we quantified the $ALDH^+$ cancer stem-like cell (CSC) population in control and treated tumors by flow cytometry. Ruxolitinib treated tumors demonstrated a trend toward decreased CSC numbers (Fig. 4D).

Finally, given the important role of IL6 and LIF signaling in inflammation, we sought to extend these in vivo findings to an immunocompetent mouse model system. We selected the ID8 intraperitoneal ovarian cancer mouse model in the C57BL/6 mouse strain [22]. Adipose-derived MSC from the syngeneic mouse strain were obtained commercially, and the expression of IL6 and LIF by these MSC assessed. Basal IL6 expression was noted in the MSC, and increased expression of both IL6 and LIF cytokines by the MSC following culture with ID8 conditioned media was noted, consistent with reciprocal tumor cell-MSC signaling

(Fig. 3F) [5, 17]. ID8 tumor cells and MSC were then co-injected intraperitoneally and one cohort treated with ruxolitinib-containing chow. Ruxolitinib therapy resulted in a statistically significant improvement in animal survival (Fig. 4E). Interestingly, the addition of MSC to this model system shortened the time to development of ascites (data not shown), consistent with the pro-tumorigenic effects of MSC seen in immunosuppressed animal systems [17]. Finally, ruxolitinib demonstrated on-target effects in this model system, with statistically significant decreased phosphorylated STAT3 in tumor cells following treatment (Fig. 4G).

Concluding Comments

LIF is secreted by CA-MSC in the ovarian cancer tumor microenvironment and functions in parallel with IL6 to promote tumor growth. Anti-IL6 therapy proved less effective than dual cytokine blockade both in vitro and in vivo in a model utilizing a human tumor microenvironment in which human stroma-derived IL6 and LIF both impact epithelial tumor cells, suggesting a potential redundancy of function of IL6 and LIF signaling through STAT3. This is consistent with clinical trial findings in phase I and phase I/II trials of the anti-IL6 antibody siltuximab [2, 7] and a phase I trial in which the anti-IL6 tocilizumab was investigated in combination with carboplatin and doxorubicin [8]. These trials demonstrated that anti-IL6 therapy is well-tolerated, however the treatment failed to have significant anti-tumor efficacy. We postulate that the lack of therapeutic efficacy may be due to redundant JAK/STAT pathway activation by the cytokine LIF, and that therapeutic strategies to block JAK-STAT activation must target shared downstream signaling components of both IL6 and LIF for greatest antitumor effect. These findings should help drive new clinical strategy design with the goal of improved clinical response.

Supplementary Material

Refer to Web version on PubMed Central for supplementary material.

Acknowledgments

The authors would like to thank Yusong Gong for her technical assistance in the beginning stages of this project. Funding for this work has been provided in part by the Women's Reproductive Health Research (WRHR) Career Development Program Award to KM (National Institutes of Health, K12 HD065257), the Department of Defense Ovarian Cancer Academy Early-Career Investigator Award to KM (DOD W81XWH-15–0194), and the generous support of the Goldberg Family.

References

1. American Cancer Society. www.cancer.org.
2. Anglesio MS, George J, Kulbe H, Friedlander M, Rischin D, Lemech C et al. IL6-STAT3-HIF signaling and therapeutic response to the angiogenesis inhibitor sunitinib in ovarian clear cell cancer. Clin Cancer Res 2011; 17: 2538–2548. [PubMed: 21343371]
3. Burgos-Ojeda D, McLean K, Bai S, Pulaski H, Gong Y, Silva I et al. A Novel Model for Evaluating Therapies Targeting Human Tumor Vasculature and Human Cancer Stem-like Cells. Cancer Res 2013.
4. Burke WM, Jin X, Lin HJ, Huang M, Liu R, Reynolds RK et al. Inhibition of constitutively active Stat3 suppresses growth of human ovarian and breast cancer cells. Oncogene 2001; 20: 79257934.
5. Coffman LG, Choi YJ, McLean K, Allen BL, di Magliano MP, Buckanovich RJ. Human carcinomaassociated mesenchymal stem cells promote ovarian cancer chemotherapy resistance via a BMP4/HH signaling loop. Oncotarget 2016; 7: 6916–6932. [PubMed: 26755648]

6. Corcoran RB, Contino G, Deshpande V, Tzatsos A, Conrad C, Benes CH et al. STAT3 plays a critical role in KRAS-induced pancreatic tumorigenesis. Cancer Res 2011; 71: 5020–5029. [PubMed: 21586612]
7. Coward J, Kulbe H, Chakravarty P, Leader D, Vassileva V, Leinster DA et al. Interleukin-6 as a therapeutic target in human ovarian cancer. Clin Cancer Res 2011; 17: 6083–6096. [PubMed: 21795409]
8. Dijkgraaf EM, Santegoets SJ, Reyners AK, Goedemans R, Wouters MC, Kenter GG et al. A phase I trial combining carboplatin/doxorubicin with tocilizumab, an anti-IL-6R monoclonal antibody, and interferon-alpha2b in patients with recurrent epithelial ovarian cancer. Ann Oncol 2015; 26: 2141–2149. [PubMed: 26216383]
9. Ding DC, Liu HW, Chu TY. Interleukin-6 from Ovarian Mesenchymal Stem Cells Promotes Proliferation, Sphere and Colony Formation and Tumorigenesis of an Ovarian Cancer Cell Line SKOV3. J Cancer 2016; 7: 1815–1823. [PubMed: 27698921]
10. Domcke S, Sinha R, Levine DA, Sander C, Schultz N. Evaluating cell lines as tumour models by comparison of genomic profiles. Nat Commun 2013; 4: 2126. [PubMed: 23839242]
11. Gritsina G, Xiao F, O'Brien SW, Gabbasov R, Maglaty MA, Xu RH et al. Targeted Blockade of JAK/STAT3 Signaling Inhibits Ovarian Carcinoma Growth. Mol Cancer Ther 2015; 14: 1035–1047. [PubMed: 25646015]
12. Hanahan D, Coussens LM. Accessories to the crime: functions of cells recruited to the tumor microenvironment. Cancer Cell 2012; 21: 309–322. [PubMed: 22439926]
13. Kenny HA, Nieman KM, Mitra AK, Lengyel E. The first line of intra-abdominal metastatic attack: breaching the mesothelial cell layer. Cancer Discov 2011; 1: 100–102. [PubMed: 22013555]
14. Kim B, Kim HS, Kim S, Haegeman G, Tsang BK, Dhanasekaran DN et al. Adipose Stromal Cells from Visceral and Subcutaneous Fat Facilitate Migration of Ovarian Cancer Cells via IL6/JAK2/STAT3 Pathway. Cancer Res Treat 2017; 49: 338–349. [PubMed: 27456942]
15. Korkaya H, Kim GI, Davis A, Malik F, Henry NL, Ithimakin S et al. Activation of an IL6 inflammatory loop mediates trastuzumab resistance in HER2+ breast cancer by expanding the cancer stem cell population. Mol Cell 2012; 47: 570–584. [PubMed: 22819326]
16. Lane D, Matte I, Rancourt C, Piche A. Prognostic significance of IL-6 and IL-8 ascites levels in ovarian cancer patients. BMC Cancer 2011; 11: 210. [PubMed: 21619709]
17. McLean K, Gong Y, Choi Y, Deng N, Yang K, Bai S et al. Human ovarian carcinoma-associated mesenchymal stem cells regulate cancer stem cells and tumorigenesis via altered BMP production. J Clin Invest 2011; 121: 3206–3219. [PubMed: 21737876]
18. Musrap N, Diamandis EP. Revisiting the complexity of the ovarian cancer microenvironment-clinical implications for treatment strategies. Mol Cancer Res 2012; 10: 1254–1264. [PubMed: 22896662]
19. Nieman KM, Kenny HA, Penicka CV, Ladanyi A, Buell-Gutbrod R, Zillhardt MR et al. Adipocytes promote ovarian cancer metastasis and provide energy for rapid tumor growth. Nat Med 2011; 17: 1498–1503. [PubMed: 22037646]
20. Pardanani A, Hood J, Lasho T, Levine RL, Martin MB, Noronha G et al. TG101209, a small molecule JAK2-selective kinase inhibitor potently inhibits myeloproliferative disorder-associated JAK2V617F and MPLW515L/K mutations. Leukemia 2007; 21: 1658–1668. [PubMed: 17541402]
21. Penuelas S, Anido J, Prieto-Sanchez RM, Folch G, Barba I, Cuartas I et al. TGF-beta increases glioma-initiating cell self-renewal through the induction of LIF in human glioblastoma. Cancer Cell 2009; 15: 315–327. [PubMed: 19345330]
22. Roby KF, Taylor CC, Sweetwood JP, Cheng Y, Pace JL, Tawfik O et al. Development of a syngeneic mouse model for events related to ovarian cancer. Carcinogenesis 2000; 21: 585–591. [PubMed: 10753190]
23. Saini U, Naidu S, ElNaggar AC, Bid HK, Wallbillich JJ, Bixel K et al. Elevated STAT3 expression in ovarian cancer ascites promotes invasion and metastasis: a potential therapeutic target. Oncogene 2017; 36: 168–181. [PubMed: 27292260]
24. Scambia G, Testa U, Benedetti Panici P, Foti E, Martucci R, Gadducci A et al. Prognostic significance of interleukin 6 serum levels in patients with ovarian cancer. Br J Cancer 1995; 71: 354–356. [PubMed: 7841052]

25. van Dam M, Mullberg J, Schooltink H, Stoyan T, Brakenhoff JP, Graeve L et al. Structure-function analysis of interleukin-6 utilizing human/murine chimeric molecules. Involvement of two separate domains in receptor binding. J Biol Chem 1993; 268: 15285–15290. [PubMed: 8325898]

26. Wang W, Kryczek I, Dostal L, Lin H, Tan L, Zhao L et al. Effector T Cells Abrogate StromaMediated Chemoresistance in Ovarian Cancer. Cell 2016; 165: 1092–1105. [PubMed: 27133165]

27. Xu S, Grande F, Garofalo A, Neamati N. Discovery of a novel orally active small-molecule gp130 inhibitor for the treatment of ovarian cancer. Mol Cancer Ther 2013; 12: 937–949. [PubMed: 23536726]

28. Ye F, Hu Y, Lu W, Zhou C, Xie X. Expression of leukaemia inhibitory factor in epithelial ovarian carcinoma: correlation with clinical characteristics. Histopathology 2008; 53: 224–228. [PubMed: 18540977]

29. Yu H, Lee H, Herrmann A, Buettner R, Jove R. Revisiting STAT3 signalling in cancer: new and unexpected biological functions. Nat Rev Cancer 2014; 14: 736–746. [PubMed: 25342631]

30. Zhou T, Georgeon S, Moser R, Moore DJ, Caflisch A, Hantschel O. Specificity and mechanism-ofaction of the JAK2 tyrosine kinase inhibitors ruxolitinib and SAR302503 (TG101348). Leukemia 2014; 28: 404–407. [PubMed: 23823659]

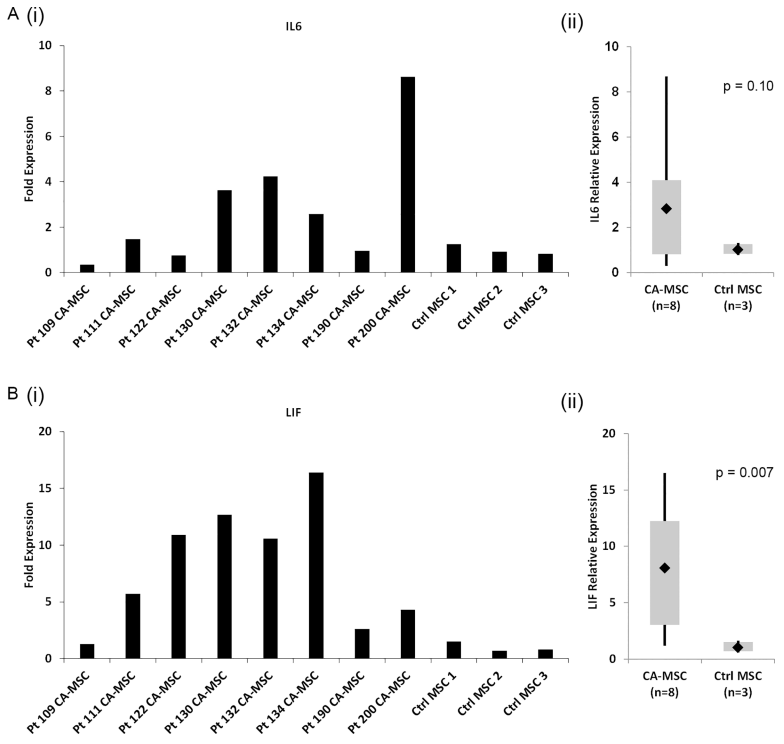

Figure 1. Cancer-associated MSC (CA-MSC) demonstrate increased levels of IL6 and LIF as compared to control MSC.

(A) Individual (i) and average (ii) IL6 mRNA expression levels by qRT-PCR in a panel of patient-derived CA-MSC and control, adipose-derived non-cancer MSC (Ctrl MSC). (B) Individual (i) and average (ii) LIF levels by qRT-PCR in the same panel of MSC. CA-MSC were isolated as previously described [17]. MSC were cultured to 80% confluence and washed once with ice-cold PBS, before being homogenized in TRizol reagent (Invitrogen) and total RNA extracted. First-strand cDNA was synthesized with the SuperScript III First-Strand Synthesis System for RT-PCR (Invitrogen). SYBR green–based array PCR was performed using the 7900 HT Sequence Detection System (Applied Biosystems). Primer amplification sequences are IL6-F (CGGGAACGAAAGAGAAGCTCTA), IL6-R (CGCTTGTGGAGAAGGAGTTCA), LIF-F (ACAGAGCCTTTGCGTGAAAC), LIF-R (TGGTCCACACCAGCAGATAA). HRPT1 was utilized for normalization, with primer sequences of HPRT1-F (ATGCTGAGGATTTGGAAAGG) and HPRT1-R (CAGAGGGCTACAATGTGATGG). The comparative Ct method was used for data analysis described at RT^2 Profiler PCR Array Data Analysis (SABiosciences). Values were normalized to average Ctrl MSC fold expression set at 1. (Aii) and (Bii) Box-and-whisker plots shown on the right demonstrate the interquartile ranges, and the diamond indicates the mean value. p-values comparing CA-MSC to control MSC calculated by 2-tailed student T test. Four to six CA-MSC lines have been used for continued experiments. Cell lines for all experiments were tested for mycoplasma contamination every 60 days.

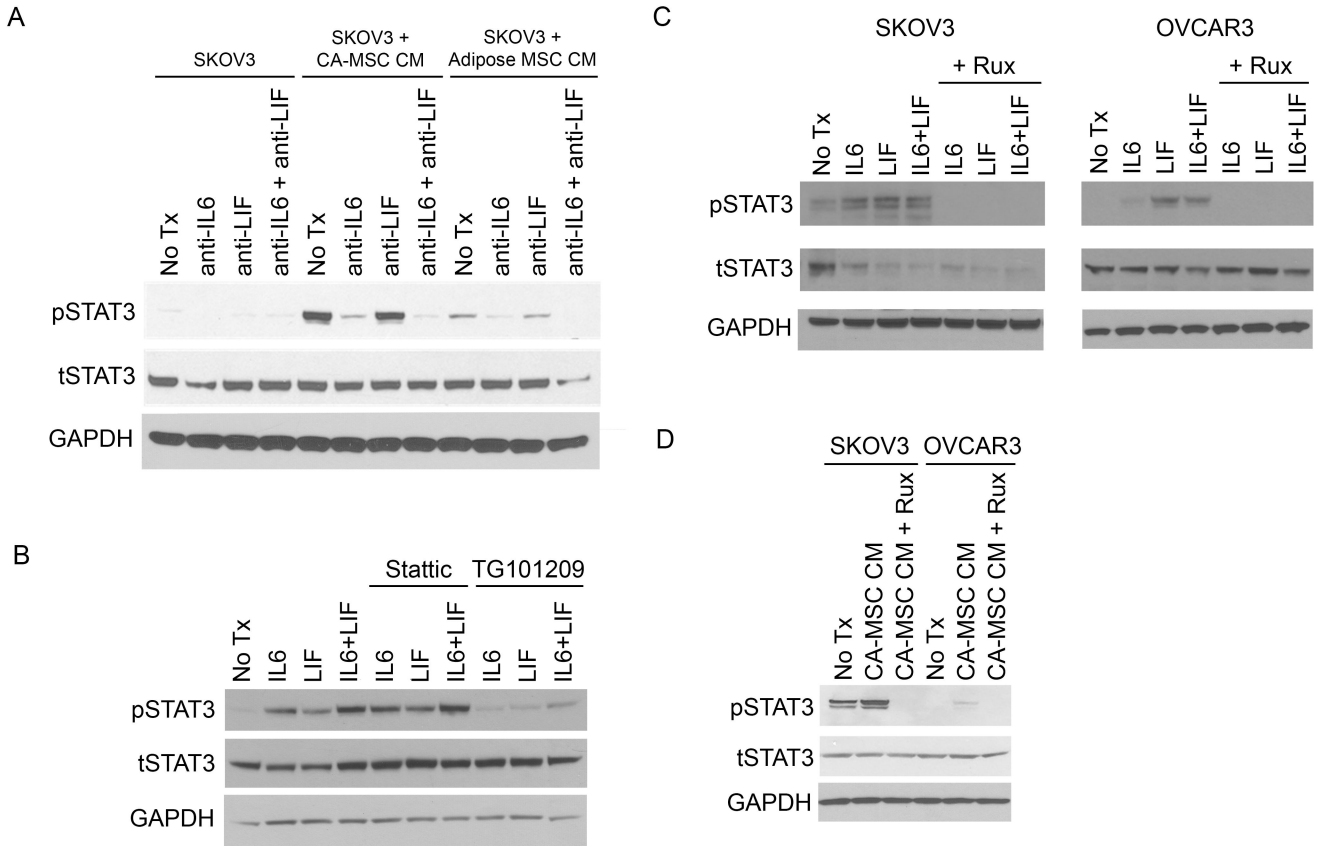

Figure 2. IL6 and LIF from CA-MSC induce cancer cell STAT3 phosphorylation that is blocked by downstream inhibitors.

(A) Immunoblot analysis demonstrating CA-MSC conditioned media induces STAT3 phosphorylation in ovarian cancer cells and this effect is blocked by anti-IL6 and anti-LIF antibodies. SKOV3 cells were cultured in the absence or presence of MSC conditioned media (MSC CM), without or with blocking antibodies of anti-IL6 (150 ng/ml, #AB-250-NA, R&D Systems) and/or anti-LIF (400 mg/ml, #AB-206-NA, R&D Systems) as indicated. Briefly, neutralizing antibodies were added to conditioned media for 2h and then media added to SKOV3 cells for 30min. Cells were then washed and cellular protein lysates obtained in RIPA buffer (Invitrogen) with complete proteinase inhibitor and phosphatase inhibitor (#1862495, Thermo Scientific). Insoluble material was removed by centrifugation. Protein concentrations were determined using the Bradford Protein Assay Kit (Bio-Rad). Lysates were separated by gel electrophoresis and transferred onto a nitrocellulose membrane. Primary antibodies for immunoblotting include anti-phospho-STAT3 (tyrosine705, #9131, Cell Signaling Technology), antitotal-STAT3 (#9139, Cell Signaling Technology) and anti-GAPDH (#2118, Cell Signaling Technology). Following incubation with the appropriate secondary antibody, bands were visualized using the ECL Kit (Thermo Scientific). (B) Immunoblot analysis evaluating the efficacy of inhibitors of the IL6-JAK-STAT signaling pathway to block IL6 or LIF mediated STAT3 phosphorylation. SKOV3 cells were pretreated with either the STAT3 inhibitor Stattic (0.3 uM, Sigma) or the JAK2 inhibitor TG101209 (0.3uM) for 2h, and then treated with recombinant IL6 (50 ng/ml, #14–8069-80, eBioscience) and/or recombinant LIF (50 ng/ml, #14–8460-80) as indicated for

24h. Lysates were then harvested and pSTAT3, tSTAT3 and GAPDH levels assessed by immunoblotting as described above. (C) Immunoblot analysis demonstrating that the anti-JAK2 small molecule inhibitor ruxolitinib inhibits both IL6 and LIF mediated induction of STAT3 phosphorylation in multiple cell lines. SKOV3 or OVCAR3 cells were pretreated with 1uM ruxolitinib (Sigma) for 2 hours and then for with recombinant IL6 and/or recombinant LIF for 24 hours. Immunoblotting was performed. (D) Immunoblot analysis demonstrating ruxolitinib inhibits CA-MSC mediated induction of STAT3 phosphorylation in multiple cell lines. Cells were mock treated or exposed to CA-MSC conditioned media without or with 1 uM ruxolitinib for 24h, and pSTAT3, tSTAT and GAPDH levels determined by immunoblotting. All experiments were performed at least twice with different CA-MSC samples.

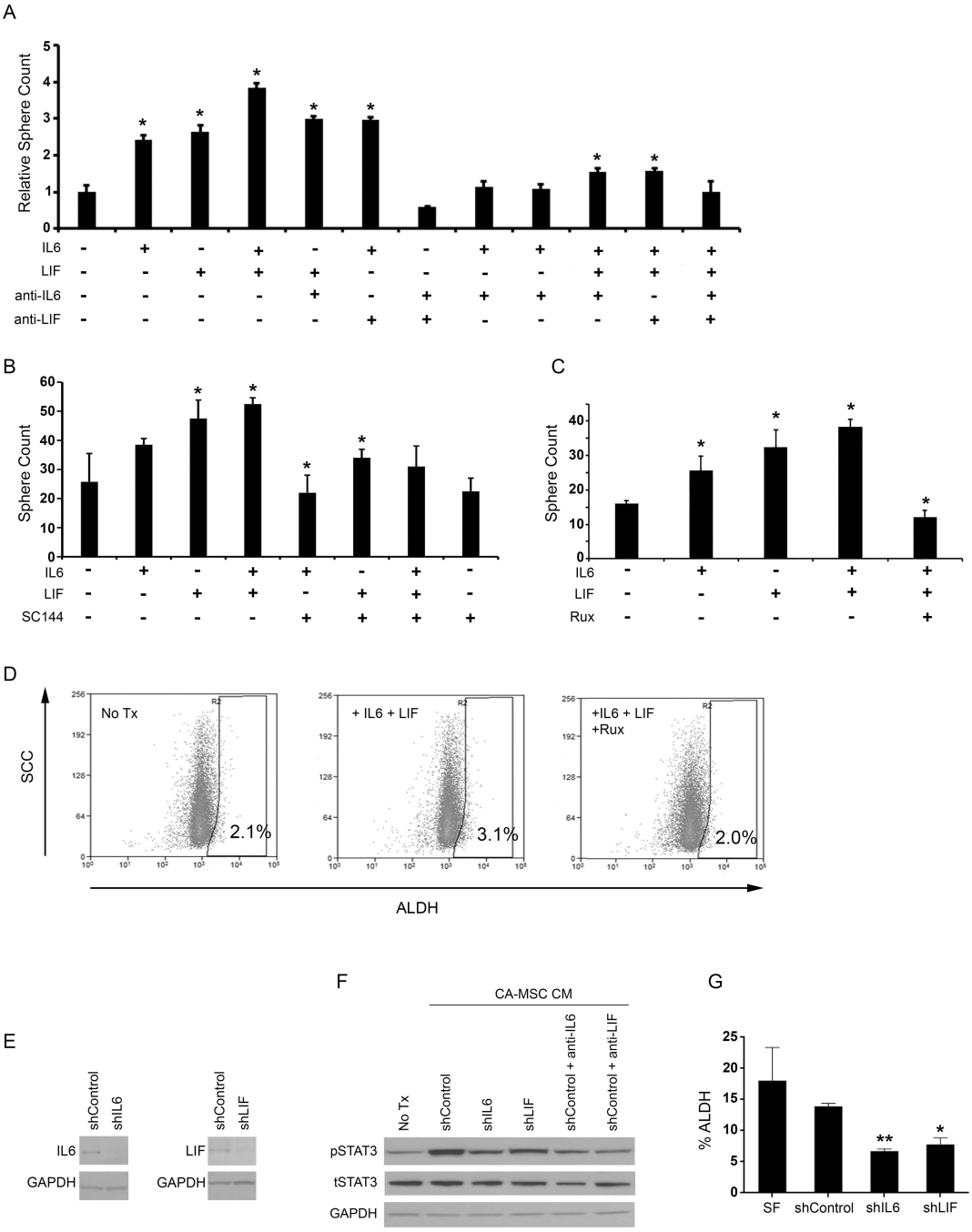

Figure 3. IL6 and LIF increase the percentage of ovarian cancer stem-like cells (CSC), and dual blockade is necessary to inhibit this effect.

Tumor sphere cell number and (B) total tumor sphere count of ovarian cancer cells following treatment with recombinant IL6 and/or LIF, and attempted blockade with individual antibody, dual antibody, or pharmacologic treatment with the GP130 inhibitor SC144. (A) A2780 cells were treated in triplicate or quadruplicate every 48h as indicated (no treatment, 50 ng/ml IL6, 50 ng/ml LIF, 150 ng/ml anti-IL6, 400 ng/ml anti-LIF). At 14 days, spheres were harvested and trypisinized, and the number of cells quantified. Sphere count was normalized to the untreated control. Bar graph heights represent mean value and error bars

indicate standard deviation. p-values were calculated using a 2-sided student T-test (* $p<0.05$). (B) SKOV3 cells were treated in triplicate every 48h for 14 days as indicated (no treatment, 50 ng/ml IL6, 50 ng/ml LIF, 0.1 uM SC144), and total spheres counted. All cell line sphere assays were performed independently at least two times and representative data are shown. Bar graph heights represent mean value and error bars indicate standard deviation. (C) Recombinant IL6 and LIF increase sphere formation in primary patient ascites-derived tumor cells, and this effect is blocked by ruxolitinib. Primary patient-derived ascites cells were treated in triplicate as indicated (no treatment, 50 ng/ml IL6, 50 ng/ml LIF, 0.25 uM ruxolitinib). Total spheres were counted at 14 days. Mean and standard deviation shown, p-values were calculated using a 2-sided student T-test (* $p<0.05$). (D) Ruxolitinib blocks IL6 and LIF mediated increase in the percentage of cancer stem like cells. SKOV3 cells were mock treated or treated with recombinant IL6 (50 ng/ml) and recombinant LIF (50 ng/ml) in the absence or presence of 1 uM ruxolitinib for 24h as indicated and the percentage of $ALDH^+$ CSC determined by the Aldefluor assay (StemCell Technologies). Representative results from multiple independent studies are shown. (E) Lentiviral-mediated shRNAs decrease IL6 and LIF expression. CA-MSC were infected with control (#SHC003V, Sigma), shIL6 (TRCN0000058587) or shLIF (TRCN0000059203) lentiviral particles at a multiplicity of infection of 1.5 and using polybrene carrier. After 48h, successfully infected cells were sorted on green fluorescent protein expression and replated for 48h. Conditioned media was collected for subsequent experiments and then GolgiStop (#51–2092KZ, BD Biosciences) added the culture media for 6 hours before harvesting cells. Lysates were separated by gel electrophoresis and transferred onto a nitrocellulose membrane. Primary antibodies for immunoblotting include anti-IL6 (#ab9324, Abcam), anti-LIF (#ab135629, Abcam) and anti-GAPDH (#2118, Cell Signaling Technology). Following incubation with the appropriate secondary antibody, bands were visualized using the ECL Kit (Thermo Scientific). (F) Conditioned media from CA-MSC following IL6 or LIF knockdown demonstrates blunted induction of STAT3 phosphorylation. SKOV3 cells were treated with conditioned media obtained from CA-MSC for 48h following shRNA lentiviral infection and sorting as described above. Anti-LIF blocking antibody (200 ng/ml, AB-250-NA, R&D Systems) and anti-IL6 blocking antibody (400 ng/ml, AB-206-NA, R&D Systems) included as positive controls. Lysates were collected and immunoblotting performed for phosphorylated STAT3, total STAT3 and GAPDH as described in Figure 2. (G)IL6 or LIF knockdown in CA-MSC prevents cytokine-mediated induction of ALDH+ CSC. SKOV3 cells were treated with conditioned media obtained from CA-MSC for 48h following shRNA lentiviral infection and sorting as described. SKOV3 cells were then harvested and the percentage of $ALDH^+$ CSC determined by the Aldefluor assay (StemCell Technologies). Mean and standard deviation shown, p-values were calculated using a 2-sided student T-test (* $p<0.05$, ** $p<0.01$) versus shControl.

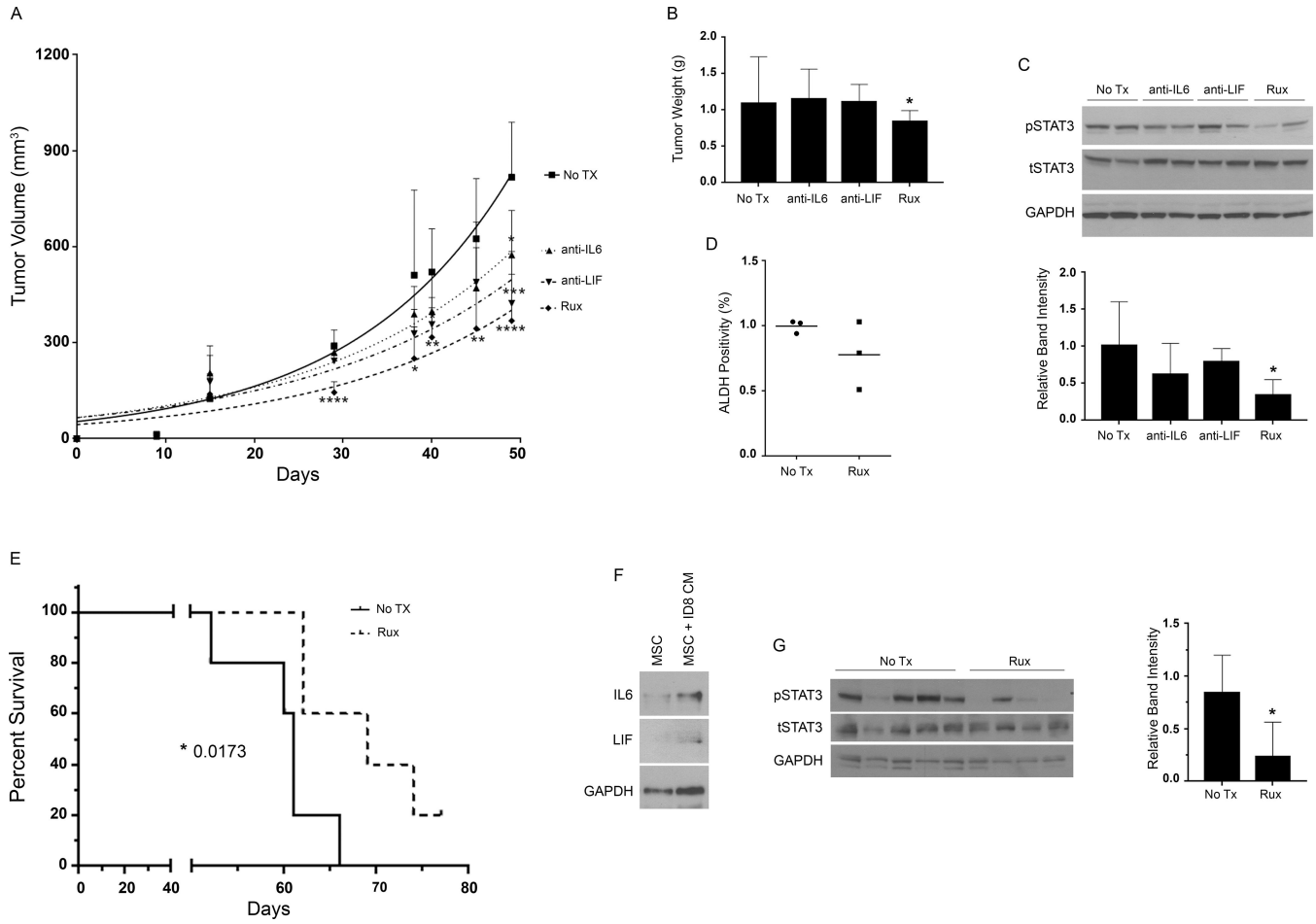

Figure 4. Dual blockade of IL6 and LIF signaling is required to abrogate CA-MSC mediated induction of xenograft tumor growth.

(A) Growth curves demonstrate decreased tumor growth over time with ruxolitinib. Female NSG mice were obtained from Jackson Laboratories. Animals were maintained in accordance with institutional policies. When the mice were approximately 6 weeks of age, 1 × 10^5 OVCAR3 (NCI-60) cells plus 1 × 10^5 CA-MSC were injected with 100 μl of growth factor-reduced Matrigel (BD Biosciences) into the bilateral axillae to generate tumors (n=8 tumors per treatment group, calculated based on 80% power to detect a 30% change in average tumor volume of 1,000 mm^3 with a standard deviation of 25% and at most 5% type I error.). All studies were done using early-passage ovarian cancer MSCs (passage 3–8). Treatment groups included were vehicle control (100 ul PBS), anti-IL6 (tocilizumab, Genentech, 10mg/kg, intraperitoneally 3x/week), anti-LIF (human LIF antibody, #AF250-NA, R&D Systems, 4ug, intraperitoneally 3x/week) and ruxolitinib chow (Incyte corporation). Tumor growth was measured using calipers, and volumes were calculated based on the modified ellipsoid formula (length × width × width/2). Investigators were not blinded to treatment groups. Statistical analysis was performed using GraphPad Prism with one-way Anova with post-hoc Tukey's test and pvalues compared to the no treatment group are indicated (* $p<0.05$, ** $p<0.01$, *** $p<0.001$, and **** $p<0.0001$). (B) Tumor weights at the time of animal sacrifice demonstrating ruxolitinib-treated animals demonstrated a

statistically significant smaller tumor size. Mean and standard deviation shown. pvalues were calculated using a 2-sided student T-test, (* $p<0.05$). (C) Immunoblot analysis of tumors demonstrating on-target effects of ruxolitinib in decreasing phosphorylated STAT3 levels. Lysates were made from tumor tissue and immunoblotting for pSTAT3 and tSTAT3 was performed as described in Figure 2. The histogram shows the mean and standard deviation of immunoblot band intensity as quantified using ImageJ (National Institutes of Health), and the intensity for each treatment group was compared to the mock-treated control using 2-tailed student T test (* $p<0.05$). (D) FACS analysis of tumors demonstrates a trend toward decreased CSC in tumors following ruxolitinib treatment. Single cells suspensions were made at the time of tumor harvest and the percentage of $ALDH^+$ cells determined by flow cytometry with the Aldefluor assay (StemCell Technologies). (E) Ruxolitinib therapy improves survival in an immunocompetent mouse model incorporating syngeneic MSC. Female C57BL/6 mice were obtained from Charles River Laboratories. Animals were maintained in accordance with institutional policies. At approximately 6 weeks of age, mice were injected intraperitoneally with 5×10^6 ID8 ovarian cancer cells plus 1.5×10^6 syngeneic mouse adipose-derived MSC suspended in PBS. Mice were randomized into two treatment groups to evenly distribute starting weights, and then either treated with ruxolitinib chow (Incyte corporation) or regular chow (n=5 per group, sample size selected empirically). Animals were monitored twice per week including animal weights, and sacrificed either at 30 g total weight or significant illness, as discussed with the animal care facility. Investigators were not blinded to treatment groups. The Kaplan-Meier survival curve is shown, and p-value of 0.0173 as calculated using the log-rank (Mantel-Cox) test. (F) Mouse adipose-derived MSC express IL6 and LIF following exposure to mouse ID8 ovarian cancer cells. Mouse adipose-derived MSC (MUBMD-01001, Cyagen) from the C57BL/6 strain were cultured in OriCell MSC growth medium (MUXMD-90011, Cyagen). ID8 conditioned media was added to the mouse MSC for 48 hours, treated with GolgiPlug (#512301KZ, BD Biosciences) for 6 hours and then lysates made and immunoblotting for mouse IL6 and LIF performed with the following primary antibodies: anti-IL6 (#229381, Abcam), anti-LIF (#ab135629, Abcam), and anti-GAPDH (#2118, Cell Signaling Technology). (G) ID8 tumors demonstrate decreased phosphorylated STAT3 levels following ruxolitinib therapy. At the time of animal sacrifice, tumor cells were collected, lysates made, and immunoblotting performed for phosphorylated STAT3, total STAT3 and GAPDH as described in Figure 2. The histogram shows the mean and standard deviation of immunoblot band intensity as quantified using ImageJ (National Institutes of Health), and relative intensity between the two groups was compared using 2-tailed student T test (* $p<0.05$).